Available online at www.sciencedirect.com
SCIENCE DIRECT®
Tetrahedron: Asymmetry
Tetrahedron: *Asymmetry* 17 (2006) 1603–1608

Diastereomeric cinchona based surfactants: features and chirality expression of their aggregates

Francesca Ceccacci,[a] Oscar Cruciani,[b] Marco Diociauti,[c] Giuseppe Formisano,[c] Luciano Galantini,[a] Wolfgang Lindner,[d] Giovanna Mancini[b,e,*] and Claudio Villani[f]

[a]*Dipartimento di Chimica, Università degli Studi di Roma 'La Sapienza', P.le A. Moro 5, Roma 00185, Italy*
[b]*CNR, Istituto di Metodologie Chimiche, Dipartimento di Chimica 'La Sapienza', P.le A. Moro 5, Roma 00185, Italy*
[c]*Istituto Superiore di Sanità, V.le Regina Elena 299, Roma 00161, Italy*
[d]*Institute of Analytical Chemistry and Food Chemistry, University of Vienna, Waehringerstrasse 38, Wien 1090, Austria*
[e]*Centro di Eccellenza Materiali Innovativi Nanostrutturati per Applicazioni Chimiche Fisiche e Biomediche, Italy*
[f]*Dipartimento di Studi di Chimica e Tecnologia delle Sostanze Biologicamente Attive, Università degli Studi di Roma 'La Sapienza', P.le A. Moro 5, Roma 00185, Italy*

Received 18 May 2006; accepted 29 May 2006

Abstract—The preparation and the aggregation properties of new diastereomeric cationic *cinchona* derivatized surfactants are described. The opposite configuration of a stereogenic center strongly influences the morphology, the colloidal features, and the chiral recognition capabilities of the diastereomeric aggregates that have been investigated by various physico-chemical tools.

1. Introduction

Chiral recognition in the cell membrane has a fundamental role in the physico-chemical features of the biological membrane as well as in intracellular trafficking governed by the membrane organization.[1] Due to the central role of biological membranes in many life processes, this recognition phenomenon may also have had a role in processes that have dictated the lack of symmetry in biomolecules.[2–4]

Chiral recognition is generally due to a complex blend of non-covalent specific interactions between chiral species. The understanding of these interactions in simple molecular complexes is not trivial and becomes extremely difficult in systems such as biological membranes that are composed of hundreds of different chiral components. The use of models such as liposomes or micellar aggregates makes investigation less demanding by modulating the level of complexity, however, a systematic work is still necessary because the interactions involved are numerous, interrelated, and depend on many parameters such as the composition of the aggregate, the molecular structure of the components and the experimental conditions.

In the context of our investigations on the discrimination of enantiomeric biarylic derivatives in chiral micellar aggregates,[5–8] we reported on the deracemization of 2′-alkoxy-2-carboxy-6-nitrobiphenyls, in aggregates formed by diastereomeric *N*-hexadecyl-*N*-methyl-L-prolinolinium bromides **1a** and **1b**.[6,7] Herein, we report on deracemization experiments carried out on racemic 2′-dodecyloxy-2-carboxy-6-nitrobiphenyl **2** in the presence of aggregates formed by either (1*S*,2*S*,4*S*,5*R*)-(+)-1-hexadecyl-5-vinyl-2-quinuclidiniume-methanol bromide **3a** or by (1*S*,2*R*,4*S*,5*R*)-(+)-1-hexadecyl-5-vinyl-2-quinuclidiniume-methanol **3b**. These surfactants, analogous to diastereomeric surfactants **1**, feature two adjacent stereogenic centers, one being the quaternary nitrogen and the other C2. Surfactants **3a** and **3b** have the same nitrogen configuration and an opposite configuration at C2, whereas surfactants **1a** and **1b** have the same configuration on the carbon and opposite on the nitrogen. Though substitution on the two stereogenic centers may be regarded as similar, the different molecular structure of surfactants **1** and **3** (including the additional

* Corresponding author. Tel.: +39 0649913078; fax: +39 06490421; e-mail: giovanna.mancini@uniroma1.it

0957-4166/$ - see front matter © 2006 Elsevier Ltd. All rights reserved.
doi:10.1016/j.tetasy.2006.05.032

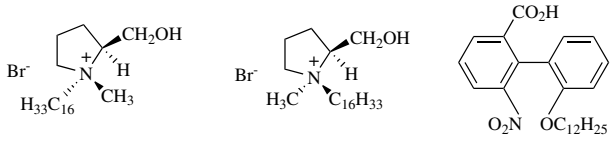

1a 1b 2

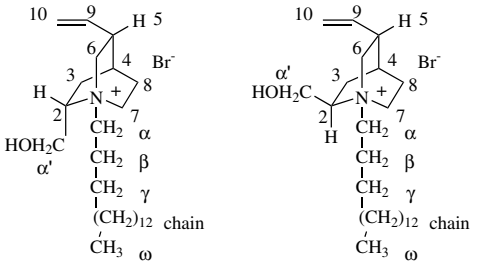

3a 3b

stereogenic centers at C4 and C5) may have dramatic effects on the organization of the aggregates and therefore on their recognition properties.

2. Results and discussion

2.1. Surfactant preparation and aggregation behavior

Surfactants **3a** and **3b** were prepared by the alkylation of (2*S*,4*S*,5*R*)-(+)-5-vinyl-2-quinuclidinemethanol and (2*R*,4*S*,5*R*)-(+)-5-vinyl-2-quinuclidinemethanol, respectively. After a complete ^{1}H and ^{13}C NMR characterization by H,H-COSY and C,H-HETCOR experiments in CD_3OD solution, their aggregating behavior in aqueous solution was investigated by LLS experiments, conductivity measurements, transmission electron microscopy, TEM, and by NMR. The main features of the aggregates formed by either **3a** or **3b** are reported in Table 1.

Conductivity measurements yielded different Krafft points and Krafft temperatures for **3a** and **3b**, as reported in Table 1. LLS experiments were performed on the aqueous solution of **3** under two different conditions, that is, 40.0 mM in surfactant in the presence of 0.2 M NaCl and 26.6 mM in surfactant in the presence of 50 mM NaBr. The choice of these conditions was imposed in one case by using the concentration of the surfactant used in the deracemization experiments, and in the other by using an added salt with the same anion of the surfactant; the combination of both conditions was not possible because it induced precipitation. At 40.0 mM concentration (at 321 K), both surfactants yield very large aggregates, whereas at 26.6 mM (at the same temperature), surfactant **3a** yields small sized aggregates and surfactant **3b** still yields large aggregates. Moreover, as shown in Figure 1, **3a** aggregate hydrodynamic radius (R_h) remains almost constant when increasing the temperature, showing the typical behavior of spherical micelles. Conversely, a marked temperature induced decrease of **3b** aggregate radius is observed, which asymptotically approaches the **3a** micelle value. According to the explanation of similar trends, as reported in the literature for other surfactants,[9] we believe that **3b** forms, at lower temperatures, rodlike aggregates that progressively reduce their length up to the formation of a spherical primary micelle. The **3b** radius asymptotic value indicates that **3a** and **3b** spherical micelles are similar, and this is reasonable because the two surfactants feature the same hydrophobic chain.

Table 1. Features of aggregates formed by surfactants **3**

Surfactant	Krafft point	Krafft temp (40.0 mM)	cmc (321 K)	R_h (321 K)
3a, 40.0 mM	309 K	316 K	$5.11 \pm 0.28 \times 10^{-4}$ M	14.0 nm[a]
3a, 26.6 mM				2.6 nm[b]
3b, 40.0 mM	296 K	304 K	$5.71 \pm 0.25 \times 10^{-4}$ M	17.0 nm[a]
3b, 26.6 mM				20.0 nm[b]

[a] In the presence of 200 mM NaCl.
[b] In the presence of 50 mM NaBr.

Both replicas and negative stained sample micrographs (Figs. 2 and 3, respectively) show clearly the presence of rods in the aqueous solutions of 40.0 mM **3b** in the presence of 200 mM NaCl. The freeze fracture micrograph shows wormlike aggregates and also the EFTEM micrograph clearly shows (in white) the shapes of worms. In both micrographs, the aggregates feature a cross section in agreement with that hypothesized on the basis of the LLS measurements at increasing temperature (Fig. 1). We believe that the obtainment of nice images by both techniques is due to the formation, under these conditions, of metastable solutions; on the other hand, it was not possible to perform analogous experiments on aqueous solutions of surfactant **3a** because of its high Krafft temperature and of its strong tendency to flocculate.

2.2. Deracemization experiments

^{1}H NMR experiments were carried out on an aqueous solution of 8.0 mM biphenylic derivative **2** and 40 mM surfactants **3**, at 321 K (well above the Krafft temperature of surfactant **3a**). ^{1}H NMR spectra show a slight loss of signal

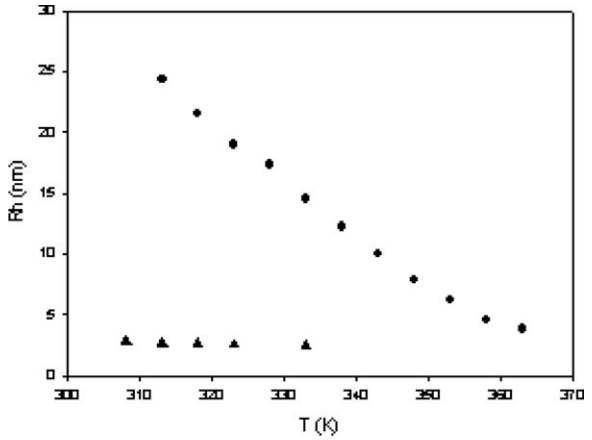

Figure 1. The mean hydrophobic radius (R_h) of aggregates formed by **3a** (triangles) and **3b** (circles) plotted as a function of temperature.

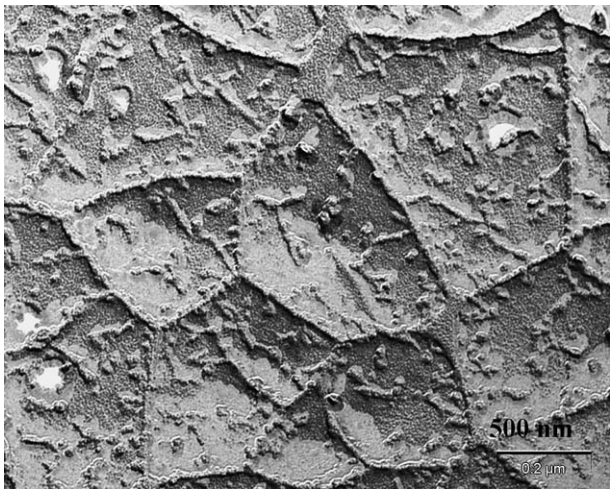

Figure 2. Freeze-fracture micrograph of a 40.0 mM aqueous solution of **3b** in the presence of 200 mM NaCl.

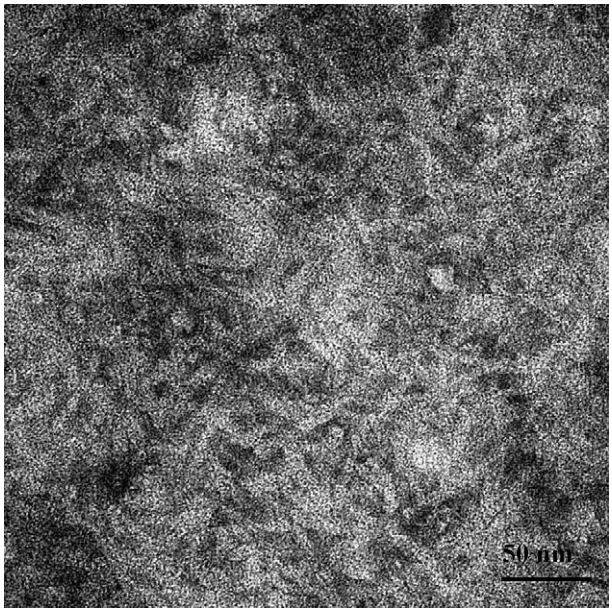

Figure 3. TEM image of a 40.0 mM aqueous solution of **3b** in the presence of 200 mM NaCl.

resolution upon association of the biphenylic derivative with the aggregates (Figs. 4 and 5). The NMR spectra obtained were not informative about chiral recognition phenomena because the diastereomeric interactions of the biphenyl enantiomers with the chiral aggregates did not yield splitting of resonances due to biphenylic protons.

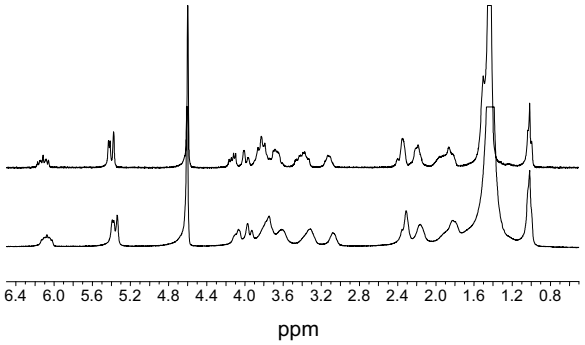

Figure 4. ^{1}H NMR spectrum of a 40.0 mM aqueous solution of surfactant **3a** in the absence (top trace) and in the presence (bottom trace) of biphenylic derivative **2**.

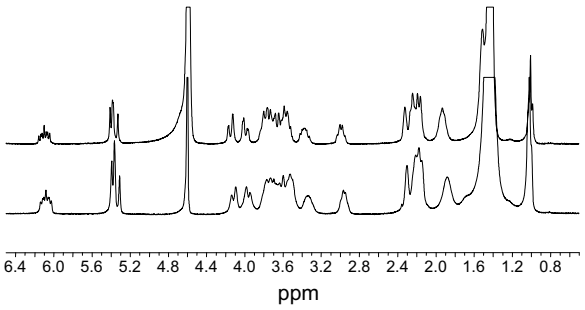

Figure 5. ^{1}H NMR spectrum of a 40.0 mM aqueous solution of surfactant **3b** in the absence (top trace) and in the presence (bottom trace) of biphenylic derivative **2**.

On the other hand, the chemical shift variation of resonances due to surfactant protons upon association of the biphenylic derivative (Table 2) gave information on the aggregation site of **2**. In fact, all resonances of surfactant **3a** are shifted upfield in the presence of the biphenylic derivative (Table 2 and Fig. 4), demonstrating that all of the surfactant protons are in the shielding cone of the aromatic system. Also, in the case of surfactant **3b** (Table 2 and Fig. 5), most resonances are shifted upfield by the interaction with the biphenylic derivative, though to a minor extent with respect to that observed for **3a**. However, signals relative to the protons of the deeper portion of the hydrophobic chain are shifted downfield, demonstrating that these protons are in the deshielding cone of the aromatic system of **2**. It is, therefore, evident that the biphenylic derivative has different sites of binding in the diastereomeric aggregates; moreover, because in both cases the biphenylic derivative is totally bound to the aggregates, due to its insolubility in water under neutral conditions, the different extent of chemical shift variation has to be

Table 2. Chemical shift variation (in ppm) of the resolved signals of surfactants **3** protons in aqueous solutions upon the addition of biphenylic derivative **2** (value of chemical shift observed in the presence of **2** is subtracted from the value of chemical shift observed in the absence of **2**)

	9	10_1	10_2	α'_1	α'_2	5	Chain	ω
3a	0.044	0.040	0.040	0.046	0.044	0.042	0.012	—
3b	0.017	0.015	0.019	0.029	0.031	0.033	−0.002	−0.011

ascribed to a different orientation of the aromatic systems with respect to the surfactant molecules.

The CD spectra performed on the same samples investigated by NMR show a negative band centered at 330 nm (Fig. 6). The band in the CD spectrum relative to the aqueous solution of **3b** is eight times more intense than the corresponding band in the spectrum relative to **3a**. It should be noted that on the basis of the CD experiments carried out on the aqueous solution of aggregates, it is not possible to assess the deracemization. It is known, in fact, that the presence of a CD band in these systems could be due to the deracemization of the biphenylic derivative, to an induced CD effect[10] or to both. We ascertained and measured deracemization by HPLC on a chiral stationary phase (ee in Table 3). HPLC experiments also allowed us to measure the extent of deracemization at a higher surfactant/biphenyl ratio (40.0 mM **3** and 0.30 mM **2**) and, therefore, to observe that the extent of deracemization increases at a lower concentration of 2 (Table 3). A different extent of the deracemization of **2** had also been observed in the presence of aggregates formed by the diastereomeric surfactants **1**,[6] where the most efficient aggregates in the deracemization of the biphenylic derivative were those formed by **1a**. However, in those aggregates the extent of deracemization was not affected by the concentration conditions.

Blank CD experiments, carried out in $CHCl_3$ solution at 40.0 mM surfactant **3** and 8.0 mM **2**, showed for both surfactant solutions negative CD bands of very low intensity (Fig. 7). Interestingly, the CD band observed in $CHCl_3$ in

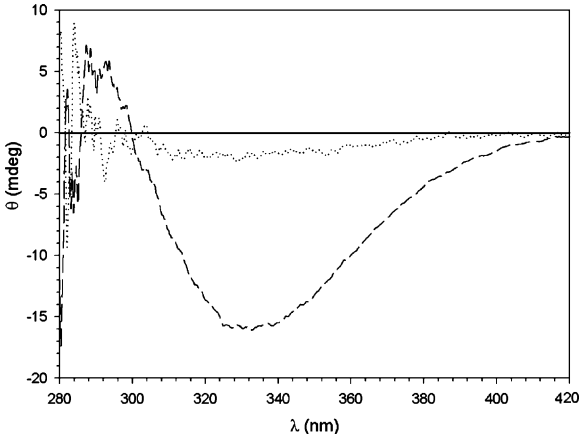

Figure 6. CD spectra of D_2O solutions of **2** in the presence of 40.0 mM **3a** (dotted line) and **3b** (dashed line).

Table 3. Enantiomeric excesses (ee) obtained in the deracemization of biphenylic derivative **2** in aggregates formed by 40.0 mM diastereomeric surfactants **3** in water and in $CHCl_3$

	ee (**2** = 8.0 mM)	ee (**2** = 0.30 mM)
3a	1% (in H_2O) 2% (in $CHCl_3$)	5% (in H_2O)
3b	8% (in H_2O) 0% (in $CHCl_3$)	11% (in H_2O)

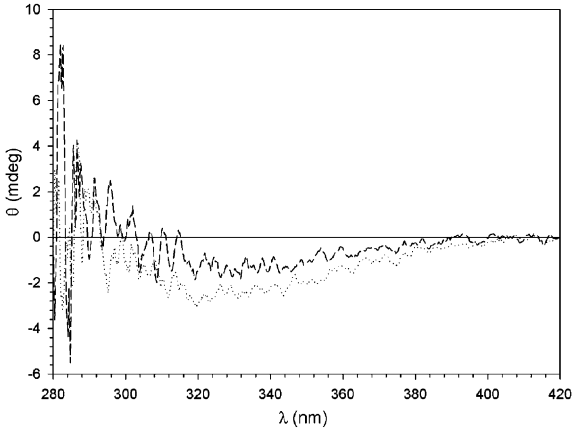

Figure 7. CD spectra of a $CHCl_3$ solution of **2** in the presence of 40.0 mM **3a** (dotted line) and **3b** (dashed line).

the presence of **3a** was more intense with respect to the band observed in the presence of **3b** (the observed ellipticity being 4 mdeg and 2 mdeg for **3a** and **3b** solutions, respectively). HPLC experiments ascertained that only in the case of surfactant **3a**, the band observed in the CD spectrum of the $CHCl_3$ solution corresponds to a deracemization process, although the resulting ee is very low. The evidence that the surfactant that is more effective in the deracemization process in $CHCl_3$ (**3a**) is less effective in aggregating conditions (in water) supports our claim[11] that chiral recognition in polymolecular aggregates is due to the aggregate as a whole or, at least, to a chiral cleft of the aggregate rather than to the interaction with a single monomer within the aggregate.

Another important point is the fact that both in aqueous and in $CHCl_3$ solutions, the diastereomeric surfactants induce an imbalance of the 1:1 equilibrium ratio of the interconverting biphenyl enantiomers toward the same enantiomer, although diastereomeric cinchona alkaloids usually behave as pseudoenantiomers,[12] in the sense that they normally give rise to opposite enantiomers in phase transfer catalyzed reactions. This evidence, in the context of the blank experiments in $CHCl_3$, demonstrates that the hydroxymethyl group of the surfactant has a minor role in interaction with the chiral probe. The same evidence, in the context of deracemization experiments under aggregating conditions (in water), has to be discussed by taking into consideration all other evidences relative to the diastereomeric aggregates. It is clear that the stereochemistry of the stereogenic center bearing the hydroxymethyl group has a major role in the aggregation behavior of surfactants **3**. The aggregate features control the site and the mode of binding of the chiral probe, although the favored enantiomer is controlled by a region of the aggregate whose chirality seems to depend on the invariant stereogenic centers. The major extent of the deracemization observed in aggregates formed by **3b**, with respect to the aggregates formed by **3a**, could be due to a more efficient interaction with the chiral probe due to the organization of the 'chiral cavity' or to the major concentration of the chiral probe in the deracemizing 'chiral cavity'. In fact, both the upfield shift of all the proton signals of the surfactant and the extent

of the shift suggest, in aggregates formed by **3a**, that the biphenylic derivative is spread in different regions of the aggregates with a certain topology, whereas, in aggregates formed by **3b**, the downfield shift of some signals and the minor extent of the shift suggest a site of binding limited to a more external region and a different topology of interaction. Therefore, the more hydrophobic region of the aggregates formed by **3a** could either lack recognition capabilities or favor the opposite enantiomer with respect to the upper region.

The results discussed above suggest a different expression of chirality in the aggregates formed by surfactants **3** with respect to that expressed by surfactant **1**.[6,7] The finding that in aggregates formed by surfactants **3**, the surfactant/biphenyl ratio influences the extent of deracemization suggests that the sites of chirality expression and, therefore, of chiral recognition are in a limited number, whereas in the aggregates formed by surfactant **1**, the structure of the aggregates is more flexible and can host, in the sites of chiral expression, a larger number of guest molecules, organized either in domains (with deracemization acting in a dominolike mode) or in more numerous and dynamic chiral clefts (probably induced by the solute).

3. Conclusions

The results discussed above evidence a major control of the stereogenic center bearing the hydroxymethyl group on the aggregating features of diastereomeric surfactants **3**. The non-covalent interactions responsible for aggregation and organization control the mode of binding of the chiral biphenylic probe, whose deracemization in aggregating conditions is induced by a whole region of the aggregates, whose shape and chirality is dictated by the organization of the aggregate.

4. Experimental

4.1. Materials

2′-Dodecyloxy-2-carboxy-6-nitrobiphenyl, **2**, was prepared as previously described.[5]

4.1.1. (1*S*,2*S*,4*S*,5*R*)-(+)-1-Hexadecyl-5-vinyl-2-quinuclidiniume-methanol bromide, 3a. (2*S*,4*S*,5*R*)-(+)-5-Vinyl-2-quinuclidinemethanol (0.50 g, 3.0 mmol) and 1-bromohexadecane (1.07 g, 3.5 mmol) were added to 5 mL of acetone. The mixture was heated at refluxing temperature for 2 days, after cooling, the obtained solid was filtered and washed with Et_2O. Recrystallization from acetone gave 0.92 g (65%) of a white solid; $[\alpha]_D^{25} = 17.2$ (*c* 4.7, MeOH). ^{1}H NMR δ (CD_3OD): 5.945 (m, 1H, H9); 5.30–5.18 (m, 2H, H10); 3.859 (m, 2H, C*H*$_2$OH); 3.82–3.30 (m, 5H, 2H7 + 1H6 + 1H2 + 1Hα); 3.195 (m, 2H, 1H6 + 1Hα); 2.882 (m, 1H, H5); 2.22–2.30 (m, 2H, 1H3 + 1H4); 2.083 (m, 2H, 2H8); 1.90–1.63 (m, 3H, 2Hβ + 1H3); 1.368 (m, 2H, 2Hγ); 1.279 (m, 24H, chain); 0.892 (t, 3Hω, $J = 6.56$) ppm. ^{13}C NMR δ (CD_3OD): 138.61, C(9); 117.82, C(10); 65.64, C(2); 63.55, C(α); 62.01, *C*H$_2$OH + C(6); 54.00, C(7); 39.42, C(5); 33.08; 30.80; 30.65; 30.58; 30.48; 30.21; 28.02, C(4); 27.64; 26.15, C(8); 24.79 C(3); 23.73, 23.21; 14.47, C(ω) ppm. Elemental analysis for $C_{26}H_{50}BrNO$: calculated C 66.08%, H 10.66%, N 2.96%; found C 66.46%, H 11.02%, N 2.94%.

4.1.2. (1*S*,2*R*,4*S*,5*R*)-(+)-1-Hexadecyl-5-vinyl-2-quinuclidiniume-methanol, 3b. (2*R*,4*S*,5*R*)-(+)-5-Vinyl-2-quinuclidinemethanol (0.50 g, 3.0 mmol) was alkylated with 1-bromohexadecane as described above for **3a**. Recrystallization from acetone gave off a white solid (65% yield). $[\alpha]_D^{25} = 77.9$ (*c* 2.2, MeOH). ^{1}H NMR δ (CD_3OD): 5.941 (m, 1H, H9); 5.26–5.17 (m, 2H, H10, $^3J_{trans} = 17.4$ Hz, $^3J_{cis} = 10.2$ Hz); 4.07–3.85 (m, 2H, C*H*$_2$OH); 3.78–3.42 (m, 6H, 2H6 + 2H7 + 1H2 + 1Hα); 3.276 (m, 1H, 1Hα); 2.810 (q, 1H, H5); 2.22–2.10 (m, 5H, 2H3 + 1H4 + 2H8); 1.826 (m, 2H, 2Hβ); 1.410 (m, 2H, 2Hγ); 1.310 (m, 24H, chain); 0.893 (t, 3Hω, $J = 6.6$) ppm. ^{13}C NMR δ (CD_3OD): 137.67, C(9); 117.79, C(10); 66.37, C(2); 62.00, C(α); 60.52, *C*H$_2$OH; 57.88 C(6); 56.44, C(7); 39.38, C(5); 33.09; 30.75; 30.67; 30.58; 30.50; 30.26; 28.19, C(4); 27.79; 25.29, C(8); 24.33 C(3); 23.73; 23.53; 14.48, C(ω) ppm. Elemental analysis for $C_{26}H_{50}BrNO$: calcd C 66.08%, H 10.66%, N 2.96%; found C 65.93%, H 10.93%, N 2.94%.

4.2. Samples for deracemization experiments

The required volume of a concentrated ethanol (or $CHCl_3$) solution of **2** was added to a fixed volume of a 40 mM D_2O (or $CHCl_3$) solution of surfactant **3**.[13] The samples were left to incubate overnight prior to measurement and were analyzed by NMR, CD, and HPLC (on a quinine *t*-butylcarbamate stationary phase[14]—250 × 4.6 mm I.D.—injecting directly the aqueous samples, eluent: methanol/acetonitrile = 60/40 + ammonium acetate 8.4 mM + acetic acid 42 mM; 283 K; flow rate 1.5 mL/min).[†]

4.3. Instrumentation

NMR spectra were recorded on a Bruker AC 300 P spectrometer operating at 300.13 and 75.47 MHz for ^{1}H and ^{13}C, respectively.

Signals were referenced with respect to TMS ($\delta = 0.000$ ppm), used as an internal standard in CD_3OD and to the residual proton signal of D_2O ($\delta = 4.4816$ at 323 K) in D_2O.

CD spectra were recorded on a Jasco spectropolarimeter J-715 using quartz cells of 0.1 cm path length. Optical rotation measurements were carried out on a Perkin Elmer-241 polarimeter.

Conductivity measurements were carried out on a Hanna conductimeter HI 9932, equipped with a thermostating apparatus.

[†] Under these HPLC conditions, the on-column interconversion rate of the enantiomers is slow compared to the separation rate, and peaks due to the two enantiomers are well resolved and their area is easily measured (see Ref. 6).

Quasi-elastic laser light scattering measurements were performed with a Brookhaven instrument, consisting of a BI-2030AT digital correlator with 136 channels and a BI-200SM goniometer. The light source was a Uniphase solid-state laser system model 4601 operating at 532 nm. Dust was eliminated by means of a Brookhaven ultra filtration unit (BIUU1) for flow-through cells, the volume of the flow cell being about 1 cm^3. Nucleopore filters with a pore size of 0.4 μm were used. The samples (prepared either 40.0 mM or 26.6 mM in **3** in the presence of 200.0 mM NaCl and 50.0 mM NaBr, respectively) were placed in the cell for at least 30 min prior to measurements to allow for thermal equilibration. Temperature was controlled by means of a circulating water bath.

Transmission electron microscopy (TEM) experiments were carried out on a energy-filtered transmission electron microscope (EFTEM) Zeiss 902, operating at 80 kV. In order to enhance the contrast, the microscope was settled to collect only elastic electrons ($\Delta E = 0$). Inelastic electrons scattered from the sample contribute only to the image background noise and their filtering out strongly enhances the final image quality.[15] The samples were prepared as follows: a droplet of the 40.0 mM aqueous solution of surfactant **3b** in the presence of 200 mM NaCl was deposited onto 300 mesh copper grids for electron microscopy covered with a very thin (about 20 nm) amorphous carbon film and the excess of liquid was removed by placing the grid on a filter paper. When the grid was dried, a droplet of the stain solution was deposited and dried by the same procedure. A negative stain was obtained with a 2% w/v solution of phosphotungstate acid (PTA) buffered at pH = 7.3 (NaOH).

Freeze fracture electron microscopy experiments were performed on a Philips EM 208S (FEI Company, Eindhoven, The Netherlands) at 60 kV. Replicas were prepared as follows: the aqueous samples **3b** (40.0 mM in the presence of 200 mM NaCl) were placed on hold carriers and quickly frozen in Freon 22, partially solidified at the liquid nitrogen temperature. The mounted carriers were then transferred into a Bal-Tec BAF 060 freeze-etch unit (BAL-TEC Inc., Balzers, Liechtenstein), cleaved at −100 °C at a pressure of $2–4 \times 10^{-7}$ mbar, shadowed with 2 nm of platinum–carbon and replicated with 20 nm carbon film. Platinum–carbon evaporation (at an angle of 45°) and carbon evaporation (at an angle of 90°) were performed using electron beam guns; the thickness of the deposit was evaluated by means of a quartz crystal thin film monitor. The samples were digested for 2 h from the replica by methanol. The replicas were mounted on naked 300-mesh grids and examined.

Acknowledgements

This work was carried out in the frame of a European project of Action COST D11 entitled 'Chiral Recognition in Self-assembled Systems'. We acknowledge contributions from CNR, Dipartimento di Progettazione Molecolare and from MIUR (PRIN 2005 contract no. 2005037725_001). Ernst Tobler, Institute of Analytical Chemistry, University of Vienna, is specifically acknowledged for the synthesis of surfactants **3**.

References

1. Lalitha, S.; Sampath Kumar, A.; Stine, K. J.; Covey, D. F *J. Supramol. Chem.* **2001**, *1*, 53–61.
2. Avalos, M.; Babiano, R.; Cintas, P.; Jiménez, J. L.; Palacios, J. C. *Tetrahedron: Asymmetry* **2000**, *11*, 2845–2874.
3. Bonner, W. A. *Chem. Ind. (London)* **1992**, *17*, 640–644.
4. Bailey, J. *Acta Astronaut.* **2000**, *46*, 627–631.
5. Bella, J.; Borocci, S.; Mancini, G. *Langmuir* **1999**, *15*, 8025–8031.
6. Borocci, S.; Ceccacci, F.; Galantini, L.; Mancini, G.; Monti, D.; Scipioni, A.; Venanzi, M. *Chirality* **2003**, *15*, 441–447.
7. Ceccacci, F.; Diociaiuti, M.; Galantini, L.; Mancini, G.; Mencarelli, P.; Scipioni, A.; Villani, C. *Org. Lett.* **2004**, *6*, 1565–1568.
8. Andreani, R.; Bombelli, C.; Borocci, S.; Lah, J.; Mancini, G.; Mencarelli, P.; Vesnaver, G.; Villani, C. *Tetrahedron: Asymmetry* **2004**, *15*, 987–994.
9. Mazer, N. A.; Benedek, G. B.; Carey, M. C. *J. Phys. Chem.* **1976**, *80*, 1075–1085.
10. Allenmark, S. *Chirality* **2003**, *15*, 409–422.
11. Ceccacci, F.; Mancini, G.; Sferrazza, A.; Villani, C. *J. Am. Chem. Soc.* **2005**, *127*, 13762–13763, and references cited therein.
12. O'Donnell, M. J.; Delgado, F.; Pottorf, R. S. *Tetrahedron* **1999**, *37*, 3183–3186.
13. Kremer, J. M. H.; van der Esker, M. W. J.; Pathmamanoharan, C.; Wiersema, P. H. *Biochemistry* **1977**, *16*, 3932–3935.
14. Tobler, E.; Lammerhofer, M.; Lindner, W.; Mancini, G. *Chirality* **2001**, *13*, 641–647.
15. Egerton, R. F. *Electron Energy Loss Spectroscopy*; Plenum Press: New York, 1986.